Kalman Filtering in Chandra Aspect Determination

Roger Hain, Thomas Aldcroft, Robert Cameron, Mark Cresitello-Dittmar, Margarita Karovska

Harvard-Smithsonian Center for Astrophysics, 60 Garden St., Cambridge, MA 02139

Abstract.
The ability of the Chandra X-Ray Observatory to achieve unprecedented image resolution is due, in part, to the ability to accurately reconstruct the spacecraft attitude history. This is done with a Kalman filter and Rauch-Tung-Striebel (RTS) smoother, which are key components of the overall aspect solution software. The Kalman filter/RTS smoother work by combining data from star position measurements, which are accurate over the long term but individually noisy, and spacecraft rate information from on-board gyroscopes, which are very accurate over the short-term, but are subject to drifts in the bias rate over longer time scales. The strengths of these two measurement sources are complementary. The gyro rate data minimizes the effects of noise from the star measurements, and the long-term accuracy of the star data provides a high-fidelity estimate of the gyro bias drift. Analysis of flight data, through comparison of observed guide star position with expected position and examination of the reconstructed X-ray image point spread function, supports the conclusion that performance goals (1.0 arcsecond mean aspect error, 0.5 arcsecond aspect error spread diameter) were met.

1. Application of Kalman Filtering in Chandra

The schematic shown in Figure 1 illustrates the basic flow of the Kalman filter design for Chandra aspect determination. The main purpose of the filter is to maintain an accurate estimate of the spacecraft angular position, or attitude, at any point in time. Together with fiducial light data for estimating spacecraft flex, this attitude estimate is used to accurately determine the source in the celestial sphere of X-rays detected by the science instruments.

The filter estimates two main quantities: error in current attitude estimate, and gyroscope drift rate. Each of these is estimated about three axes, resulting in six estimated quantities referred to as the filter "state". The schematic illustrates the basic flow of the filter. Beginning with an initial state estimate, and initial statistics which characterize how well the state estimates are known (the "covariance"), the filter iterates through two steps.

First, as shown in the upper left box, gyro data is received. The state estimate of gyro bias is subtracted from the raw gyro data, and the spacecraft attitude is updated according to the angular motion derived from the corrected gyro data. The error statistics associated with the state are also updated, since uncertainty in gyro bias grows over time, and attitude errors due to rate uncertainty also increase. In this way, state and attitude estimates are maintained and propagated forward in time until a star camera measurement is available.

The second step is shown in the upper right box. A measurement (the location of a guide star) is received from the aspect camera and incorporated into the filter's state estimates and error statistics. The filter mathematically compares the new attitude estimate based on the current measurement with the expected attitude from the prior propagation step. The error statistics of the expected attitude and the expected error of the measurement (the noise from the star camera) are taken into account, and new estimates of attitude error and gyro bias drift are calculated. Since more data leads to a more accurate attitude estimate, the error statistics are updated to reflect more accurate attitude knowledge, and the cycle begins again with additional gyro data.

The two charts in Figure 2 show the aspect pipeline Kalman filter performance on test data, not flight data, and illustrate the behavior of the filter over time. In the upper left graph, the solid line shows actual error in pitch attitude estimate for a 500 second nominal dither observation. The dashed lines represent the root mean square (RMS) value of the covariance for pitch error (i.e., the filter's own estimate of how accurate approximately 2/3's of yaw estimates will be). Note that in this plot and the similar plot yaw estimate error plot below it, the error in each axis quickly converges to a steady state value. The two charts shown on the right demonstrate the improvement in yaw and pitch estimate error with the addition of a smoothing algorithm. The use of a smoother is possible in the aspect determination system since it is not necessary to calculate the best estimate in real time. The smoother allows better overall estimates by utilizing state and measurement data from the entire time period to improve the estimate at each point in time. The filter alone is not able to use future data to estimate at any given time. The improvements with a smoother are smaller overall attitude error and much improved performance in the very early part of the data, as seen by the much smaller RMS values.

2. Measuring Aspect Performance

To quantify overall aspect quality, a 50,000 second observation was examined. A point source was identified in this observation, and a circular region around the point source with a radius of approximately 2 arcsecond was isolated. Aspect corrected coordinates were then examined in a coordinate system aligned with the spacecraft reference frame. This coordinate system is chosen since residual aspect errors are expected to be most visible near the dither frequency, and such errors are more clearly visible as a single frequency oscillation in coordinates. The corrected sky coordinates did not show any visible oscillations, but the amount of noise is large compared to potentially small amplitude oscillations. In an attempt to remove noise due to background events to make small amplitude oscillations more visible, the data were phase modulated at the dither frequency. This was done by resetting event times to "time mod(dither period)".

The phase modulated data are shown in Figure 3. Time only goes from 0 to the dither period, and events later than an integer number of dither periods

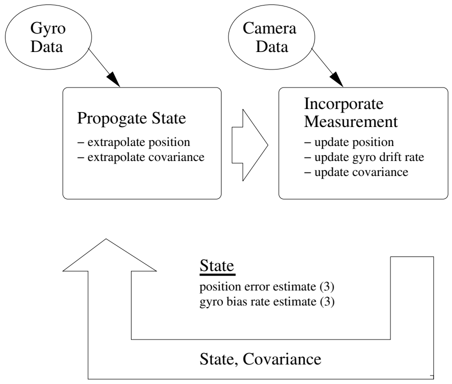

Figure 1. Chandra Aspect Kalman Filter Schematic

are wrapped back to start at time 0 again. In this way, any residual aspect error at the dither frequency is preserved in the data, but random noise can be reduced by averaging. The top charts show phase modulated data for the sky coordinates transformed to the spacecraft X axis (left) and spacecraft Y axis (right).

The two lower charts show the same data binned on 50 second intervals, with the intention of reducing noise. Ideally, if no residual oscillation were present, it would be expected that the binned data points would become smaller and smaller as the bin size becomes larger, without showing any noticeable constant offset. If, on the other hand, a clear sinusoidal signal were present, this should become apparent in the structure of the binned data points. Although even the worst case binned data point is very small (less than 0.08 arcseconds), some slight evidence of a residual signal may be present in the Y coordinate charts. The binned data shows a disproportionate number of positive data points in the first half of the dither interval, and a disproportionate number of negative data points in the second half. Note, however, that even if this error is entirely due to aspect error and not noise, the worst case still compares very favorably with the 0.5 arcsecond spread diameter requirement.

This project is supported by the Chandra X-ray Center under NASA contract NAS8-39073.

References

Gelb, A., Applied Optimal Estimation, MIT Press, Cambridge, MA, 1974

Aldcroft, T., Karovska, M., Cresitello-Dittmar, M., Cameron, R., Markevitch, M. 2000, Initial Performance of the Aspect System on the Chandra Observatory, Proc. SPIE Vol. 4012, p. 650-657, July, 2000

TRW Memorandum on AXAF Attitude and Aspect Determination, 52100.300.087 TRW-SE11K. January 11, 1996

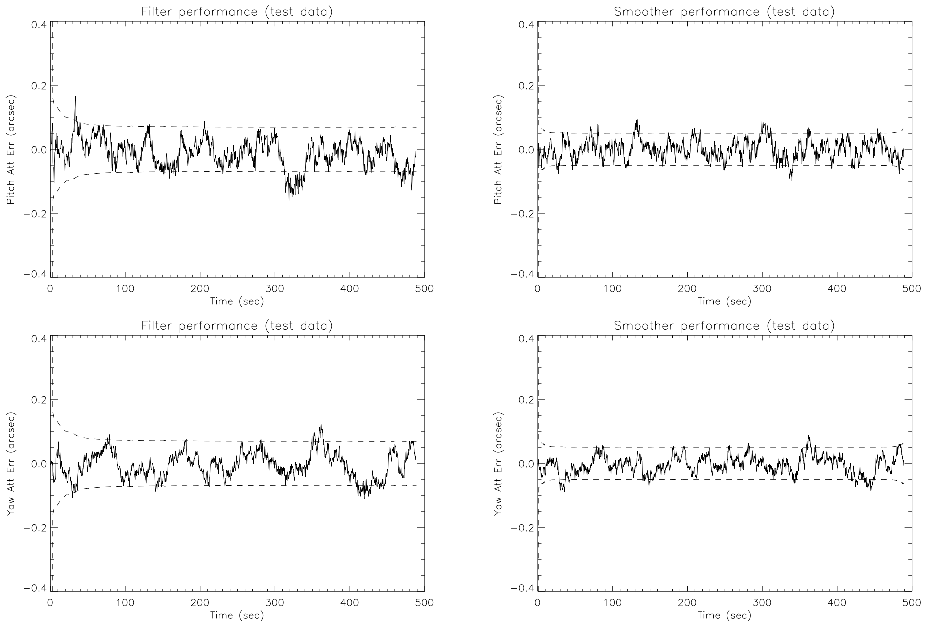

Figure 2. Sample filter and smoother results

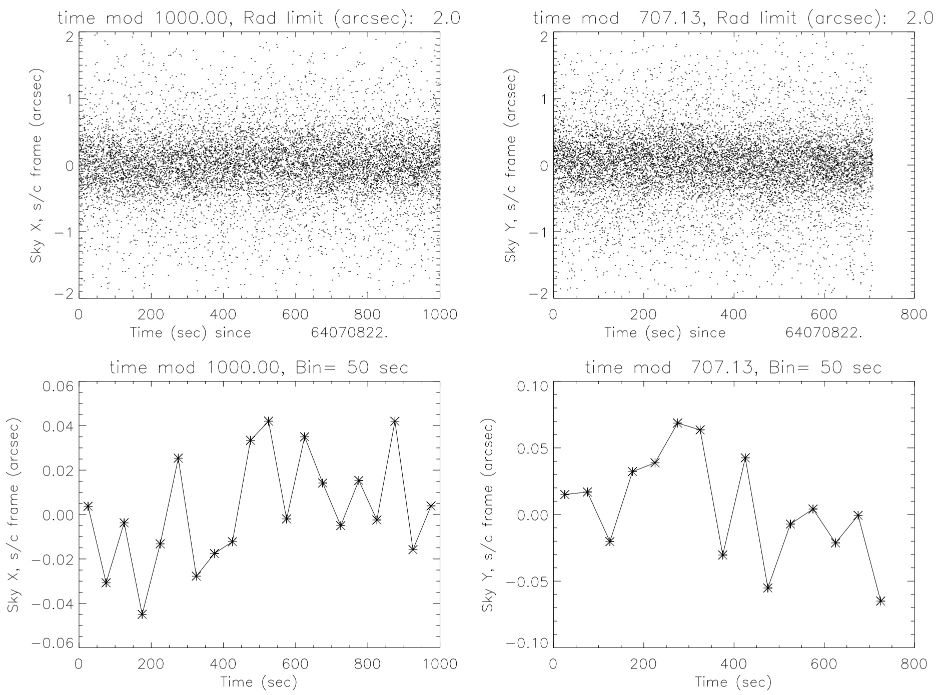

Figure 3. Aspect error in event reconstruction